Frame Design and Throughput Evaluation for Practical Multiuser MIMO OFDMA Systems

Yong-Up Jang, *Member, IEEE*, Jingon Joung, *Member, IEEE*,
Won-Yong Shin, *Member, IEEE*, and Eui-Rim Jeong, *Member, IEEE*

***Abstract*—This paper describes the design of a time-division duplexing frame with a variety of pilots for multiuser multiple-input–multiple-output orthogonal frequency-division multiple access (MU-MIMO OFDMA) systems, where the base station and users are equipped with four and two transmitting and receiving antennas, respectively. In addition, a simplified scheduling algorithm for the MU-MIMO OFDMA is proposed, and its computational complexity is analyzed. The proposed scheduling algorithm shows comparable sum achievable rates to the optimal MU-MIMO OFDMA scheduling that searches for user pairs in an exhaustive manner, whereas its complexity is fairly reduced. Furthermore, to verify the performance of MU-MIMO OFDMA systems that employ the proposed frame structure and scheduling algorithm, a system-level comparison of the average cell throughputs between the proposed MU-MIMO and the conventional MIMO OFDMA systems is numerically performed in a practical cellular environment. As a result, vital information on how we can apply MU-MIMO OFDMA schemes in cellular environments is provided.**

***Index Terms*—Cell throughput, multiuser multiple-input multiple-output (MU-MIMO), orthogonal frequency-division multiple access (OFDMA), scheduling, sum achievable rates, time-division duplexing (TDD).**

I. Introduction

In company with fundamental studies on multiple-input–multiple-output (MIMO) techniques for single transmitter and receiver [1], [2], MIMO applications for multiuser (MU) communications have vigorously been researched to further increase system throughput. For downlink (DL) MU communications, when the DL broadcasting channel-state information (CSI) is available at the transmitter, it has been shown that the capacity bound of Gaussian MIMO broadcast channels can be achieved by dirty-paper coding [3]. In cellular networks, communications from the base station (BS) to the user equipment (UE) or, simply, users are referred to as a DL [*vice versa*, uplink (UL)]. Practical implementation issues have also been studied in the area through source–channel coding in the dirty-paper channels [4]. For simple transceivers, various suboptimal techniques have been studied, e.g., linear processing methods (including channel inversion and its modifications) [5], [6], zero-forcing (ZF)-based block diagonalization [7]–[10], and minimum mean square error (MMSE)-based transmit and receive processing [11]. Note that the MU-MIMO in a flat-fading channel can easily be extended to the frequency-selective channel by employing orthogonal frequency-division multiple access (OFDMA). The combination of MU-MIMO and OFDMA converts a broadband MU-MIMO channel into parallel narrowband MU-MIMO channels [12].

The aforementioned MU-MIMO schemes, however, assume that both the transmitter and the receiver know the perfect CSI with no concerns about any channel estimation errors that occurred in practice. In time-division duplexing (TDD) cellular systems, the BS and UE generally estimate the DL CSI by using UL and DL pilot signals, respectively.[1] To relax the perfect CSI condition, a partial CSI feedback scheme using a codebook, which is made by random vector quantization, has been introduced in [13] and extended to the user selection scenario described in [14]. Opportunistic beamforming has also been studied in [15] and [16], where the precoding vector indices and signal-to-interference-plus-noise ratio (SINR) values of each user are fed back to the BS as partial CSI. Recently, for MU-MIMO systems, the achievable rate has been analyzed with channel estimation [17].

The performance of partial CSI feedback schemes is obviously inferior to perfect CSI schemes. Hence, the MU-MIMO techniques may not guarantee more throughput compared to MIMO techniques due to the interuser interference (IUI) that arises from CSI uncertainty and the system overhead required for the acquisition of the (partial) CSI. In particular, the general resource allocation in terms of frequency-and-time and user scheduling for MU-MIMO OFDMA has not been considered.[2] It would therefore be fruitful to take into

Manuscript received November 2, 2010; revised March 13, 2011 and May 24, 2011; accepted May 27, 2011. Date of publication June 23, 2011; date of current version September 19, 2011. The review of this paper was coordinated by Prof. G. Bauch.

Y.-U. Jang is with the Korea Advanced Institute of Science and Technology Institute for Information Technology Convergence, Daejeon 305-701, Korea (e-mail: yongup.jang@gmail.com).

J. Joung is with the Institute for Infocomm Research, Agency for Science, Technology and Research, Singapore 138632 (e-mail: jgjoung@i2r.a-star.edu.sg).

W.-Y. Shin is with the School of Engineering and Applied Sciences, Harvard University, Cambridge, MA 02138 USA (e-mail: wyshin@seas.harvard.edu).

E.-R. Jeong is with the Division of Information Communication and Computer Engineering, Hanbat National University, Daejeon 305-719, Korea (e-mail: erjeong@hanbat.ac.kr).

Color versions of one or more of the figures in this paper are available online at http://ieeexplore.ieee.org.

Digital Object Identifier 10.1109/TVT.2011.2160377

[1] For frequency-division duplexing systems, the DL CSI can be estimated at the UE and fed back from the UE to the BS after quantization.

[2] Note that the MU scheduling for MU-MIMO in the spatial domain has extensively been studied in [18]–[22].

account practical CSI estimation issues with realistic resource allocation methods. To the best of our knowledge, system-level performance evaluation with the channel estimation of UL and DL and with the resource allocation has not been demonstrated for the MU-MIMO OFDMA systems, and this case has motivated our study.

In this paper, cell throughputs of the proposed MU-MIMO OFDMA system and the conventional MIMO OFDMA system are compared considering CSI uncertainty and system overhead. The overall TDD frame and several pilot structures are designed for the practical MU-MIMO OFDMA systems, where the BS and users are equipped with four and two transmitting and receiving antennas, respectively, e.g., next-generation mobile Worldwide Interoperability for Microwave Access (WiMAX) [23] (IEEE 802.16m standard [24]), which is considered one of the international mobile telecommunications (IMT)-advanced technologies [25], and Third-Generation Partnership Project Long Term Evolution (3GPP LTE) advanced [26].[3] In the design framework, linear processing is considered for MU transceivers with comparatively low complexity, which results in easier implementation.

First, we employ a UL pilot-sharing technique [27] to improve the mean square error (MSE) performance of UL channel estimation. In addition to UL pilots, UL sounding pilots [28]–[30] are adaptively allocated to UEs. Note that UL pilots are used for the BS to estimate the UL CSI, whereas UL sounding pilots can be inserted into the UL subframe to select DL UEs [31], i.e., scheduling users. Existing orthogonal DL pilots with some modifications are employed to estimate plain DL channels. To estimate an *effective* DL channel, which consists of plain DL channel matrices, and MU-MIMO preprocessing and postprocessing matrices, we design the *midamble* enabling reduction of overhead.

Next, we design a suboptimal scheduling algorithm that jointly selects UEs and their spatial multiplexing modes. Using a trimming (TR) search [33] based on sequential stack search [32], the proposed scheduling algorithm can significantly reduce the computational complexity at the BS. This fact is verified from numerical and analytical comparison with an optimal exhaustive (EX)-search method.

Finally, the MU-MIMO OFDMA system with the designed frame structure and TR-search algorithm is compared with the existing MIMO OFDMA system using a closed-loop beamforming plus spatial multiplexing (CL-BFSM) [37]. The optimal number of CSI-reporting users in terms of cell throughput is observed according to the UL SINR. Because the users occupy orthogonal subcarriers on the restricted UL band for UL sounding, it has been found that, as the number of CSI-reporting users increases, the number of UL sounding pilots for each user decreases, and the CSI uncertainty subsequently increases. Therefore, the DL throughput can decrease, even if the MU diversity increases as the number of users increases.This paper can be summarized as follows.

- *Design of the MU-MIMO OFDMA TDD frame*.[4] UL sounding pilots in [28]–[30] are adaptively allocated to multiple users. The DL pilot structure with some modifications in [24] is used to increase the spectral efficiency. The DL midamble is designed to estimate effective MU DL channels and to reduce the overhead.
- *Design of the practical MU scheduling algorithm*. The TR-search algorithm in [33] is generalized.
- *Evaluation of the system-level cell throughput*. Cell throughputs of the existing MIMO and the proposed MU-MIMO OFDMA systems are compared under the cellular environment. It is corroborated that the proposed MU-MIMO OFDMA system always outperforms the existing MIMO OFDMA system.

Section II shows the MU-MIMO OFDMA system model. In Section III, the designed TDD frame and some pilot structures are described, whereas channel estimation schemes for various CSI are shown. Section IV presents our proposed scheduling algorithm. The system throughput is evaluated through a computer simulation in Section V. Finally, Section VI summarizes this paper with some concluding remarks.

Notation: Throughout this paper, the superscripts T and $*$ denote the transpose and the conjugate transpose, respectively, of a matrix. $\mathrm{tr}(\mathbf{A})$ and $\det(\mathbf{A})$ represent, respectively, a trace and a determinant of matrix $\mathbf{A}$. $\mathbb{C}^{m\times n}$ and $\mathbb{R}^{m\times n}$ are $m \times n$ complex and real matrices, respectively. The base of all logarithms is assumed to be two, unless specifically noted otherwise.

II. Multiuser Multiple-Input–Multiple-Output Orthogonal Frequency-Division Multiple Access System Model

An MU-MIMO OFDMA DL system model with one BS and T users is illustrated in Fig. 1. We assume that the BS has N_T antennas and each user has N_R antennas. The MU-MIMO technique is applied to Q orthogonal frequency bands known as MU-MIMO adaptive modulation and coding (AMC) bands. In this section, we mainly focus on a subcarrier, under the assumption that the same MU-MIMO scheme is applied to every subcarrier. Assuming that the impulse response that is sampled from a time-domain channel is shorter than the cyclic prefix, the equivalent frequency-domain channel matrix for the nth subcarrier of the kth user ($k \in \{1, \cdots, T\}$) can be represented as $\mathbf{H}_k(n) \in \mathbb{C}^{N_R\times N_T}$, which is represented by the sequential multiplication of N-point inverse discrete Fourier transform (IDFT), time-domain channel response, and N-point discrete Fourier transform (DFT) matrices. Suppose that the entries of $\mathbf{H}_k(n)$ are independent and identically distributed zero-mean complex Gaussian random variables with variance that is determined by the large-scale propagation path loss and shadowing between the BS and the UE. The BS estimates the UL channels, $\hat{\mathbf{H}}^T_{\mathrm{BS},k}(n) \in \mathbb{C}^{N_T\times N_R}$, from T users and obtains

[3]The baseline configuration for 3GPP LTE is two transmitting and receiving antennas in both the BS and the UE. Note that, in 3GPP LTE-Advanced, the existing MIMO technologies are extended to support configuration with up to eight and four transmitting and receiving antennas in the BS and the UE, respectively.

[4]DL and UL subframe structures follow the structures in [24]. We have employed the UL pilot structure as proposed in [27].

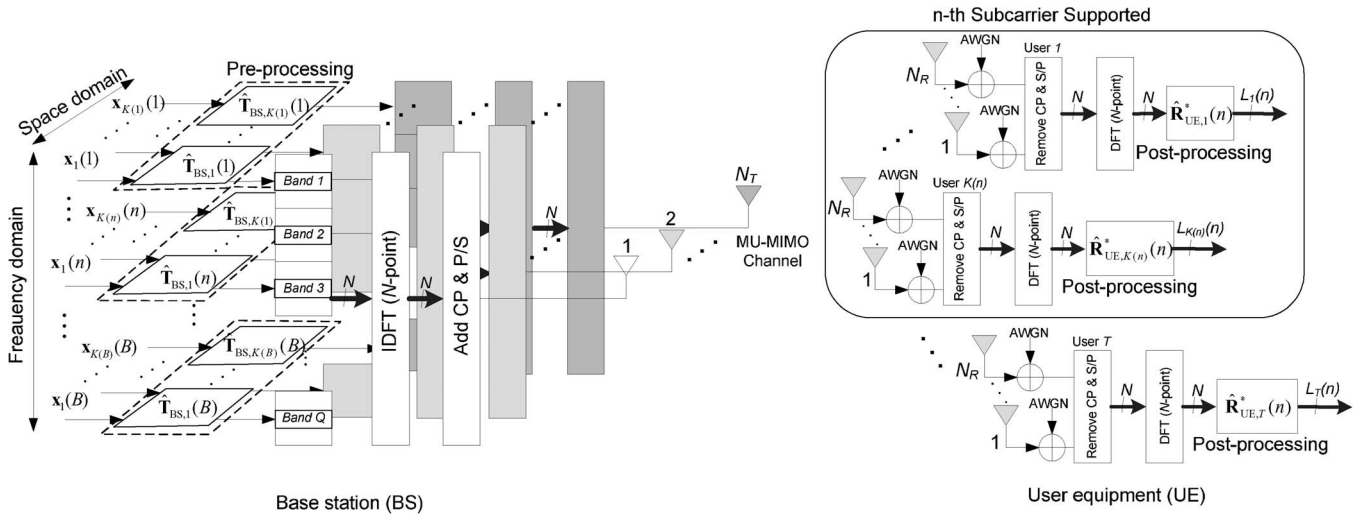

Fig. 1. MU-MIMO OFDMA system model for DL communication.

the equivalent estimated DL channels $\hat{\mathbf{H}}_{\mathrm{UE},k}(n)$ from the channel reciprocity, i.e., $\hat{\mathbf{H}}_{\mathrm{UE},k}(n) = \hat{\mathbf{H}}_{\mathrm{BS},k}(n)$, for all users $k \in \{1, \cdots, T\}$ (where the UL channel estimation procedure and method are specifically shown in Section III-B). Denoting $L_k(n)$ as the number of data streams for the nth subcarrier of the kth user, the ZF-based MU-MIMO transmit-processing matrix $\hat{\mathbf{W}}_{\mathrm{BS},k}(n) \in \mathbb{C}^{N_T \times (N_T - \sum_{j=1, j\neq k} L_j(n))}$, which suppresses the IUI, is obtained as follows [8], [9]:

$$\hat{\mathbf{W}}_{\mathrm{BS},k}(n) = \mathrm{null}\Big[\hat{\mathbf{H}}^*_{\mathrm{BS},1}(n)\hat{\mathbf{F}}_{\mathrm{BS},1}(n)\cdots\hat{\mathbf{H}}^*_{\mathrm{BS},k-1}(n)\hat{\mathbf{F}}_{\mathrm{BS},k-1}(n) \hat{\mathbf{H}}^*_{\mathrm{BS},k+1}(n)\hat{\mathbf{F}}_{\mathrm{BS},k+1}(n)\cdots\hat{\mathbf{H}}^*_{\mathrm{BS},K(n)}(n)\hat{\mathbf{F}}_{\mathrm{BS},K(n)}(n)\Big]^* \quad (1)$$

where $K(n)$ is the number of users supported at the nth subcarrier, $\mathrm{null}(\mathbf{A})$ is a matrix whose column vectors are orthogonal bases of the nullspace of $\mathbf{A}$, and the prereceiver filter matrix $\hat{\mathbf{F}}_{\mathrm{BS},k}(n)$ [7] consists of $L_k(n)$ dominant left singular vectors of $\hat{H}_{\mathrm{BS},k}(n)$. Accordingly, the kth user's input signal vector $\mathbf{x}_k(n) \in \mathbb{C}^{L_k(n)\times 1}$ is multiplied by $\hat{\mathbf{T}}_{\mathrm{BS},k}(n)$, where $\hat{\mathbf{T}}_{\mathrm{BS},k}(n) = \hat{\mathbf{W}}_{\mathrm{BS},k}(n)\hat{\mathbf{V}}_{\mathrm{BS},k}(n)\hat{\mathbf{E}}_{\mathrm{BS},k}(n)$ are combined to yield $\sum_{j=1}^{K(n)} \hat{\mathbf{T}}_{\mathrm{BS},j}(n)\mathbf{x}_j(n)$ and are broadcast. Here, the preprocessing matrix $\hat{\mathbf{V}}_{\mathrm{BS},j}(n)$ and the power control matrix $\hat{\mathbf{E}}_{\mathrm{BS},j}(n)$ are described in the following discussion. After multiplying the received signal with a postprocessing matrix $\hat{\mathbf{R}}^*_{\mathrm{UE},k}(n) = \hat{\mathbf{U}}^*_{\mathrm{UE},k}(n)\hat{\mathbf{F}}^*_{\mathrm{UE},k}(n) \in \mathbb{C}^{L_k(n)\times N_R}$, the postprocessed signal vector $\tilde{\mathbf{x}}_k(n)$ at the kth user is given by

$$\tilde{\mathbf{x}}_k(n) = \hat{\mathbf{R}}^*_{\mathrm{UE},k}(n)\mathbf{H}_{\mathrm{UE},k}(n)\sum_{j=1}^{K(n)} \hat{\mathbf{W}}_{\mathrm{BS},j}(n)\hat{\mathbf{V}}_{\mathrm{BS},j}(n) \times \hat{\mathbf{E}}_{\mathrm{BS},j}(n)\mathbf{x}_j(n) + \hat{\mathbf{R}}^*_{\mathrm{UE},k}(n)\mathbf{n}_k(n) \quad (2)$$

where $\mathbf{H}_{\mathrm{UE},k}(n) \in \mathbb{C}^{N_R \times N_T}$ denotes the actual DL channel of the kth user, and $\mathbf{n}_k(n) \in \mathbb{C}^{N_R \times 1}$ denotes the sum of an additive white Gaussian noise (AWGN) and intercell interferences with variance σ_k^2.[5] Here, the combining matrix $\hat{\mathbf{F}}_{\mathrm{UE},k}(n) \in \mathbb{C}^{N_R \times L_k(n)}$ consists of $L_k(n)$ dominant left singular vectors of the estimated DL channel $\hat{H}_{\mathrm{UE},k}(n)$. The postprocessing matrix $\hat{\mathbf{U}}^*_{\mathrm{UE},k}(n) \in \mathbb{C}^{L_k(n)\times L_k(n)}$ and the preprocessing matrix $\hat{\mathbf{V}}_{\mathrm{BS},k}(n) \in \mathbb{C}^{(N_T - \sum_{j=1, j\neq k} L_j(n))\times L_k(n)}$ for the diagonalization of the kth user's MIMO channel are obtained from the left and right singular matrices of $\hat{\mathbf{F}}^*_{\mathrm{UE},k}(n)\mathbf{H}_{\mathrm{UE},k}(n)\hat{\mathbf{W}}_{\mathrm{BS},k}(n)$ and $\hat{\mathbf{F}}^*_{\mathrm{BS},k}(n)\hat{\mathbf{H}}_{\mathrm{BS},k}(n)\hat{\mathbf{W}}_{\mathrm{BS},k}(n)$, respectively. $\hat{\mathbf{E}}_{\mathrm{BS},k}(n) \in \mathbb{R}^{L_k(n)\times L_k(n)}$ is a diagonal matrix that controls the transmission power of spatial streams. We assume that equal power is loaded on each spatial stream for simplicity and $\hat{\mathbf{E}}_{\mathrm{BS},k}(n) = P_T / \sum_{j=1}^{K(n)} L_j(n)\mathbf{I}_{L_k(n)}$, where P_T is the total transmitting power of the BS. Assuming that the transpose of the estimated UL channel $\hat{\mathbf{H}}^T_{\mathrm{BS},k}(n)$ is the same as the actual DL channel $\mathbf{H}_{\mathrm{UE},k}(n)$, i.e., $\hat{\mathbf{H}}_{\mathrm{BS},k}(n) = \hat{\mathbf{H}}_{\mathrm{UE},k}(n)$, the IUI can perfectly be canceled, and (2) can then be approximated as

$$\tilde{\mathbf{x}}_k(n) \simeq \hat{\mathbf{U}}^*_{\mathrm{UE},k}(n)\hat{\mathbf{H}}_{\mathrm{EF},k}(n)\hat{\mathbf{V}}_{\mathrm{BS},k}(n)\frac{P_T}{\sum_{j=1}^{K(n)} L_j(n)}\mathbf{x}_k(n) + \hat{\mathbf{R}}^*_{\mathrm{UE},k}(n)\mathbf{n}_k(n) \quad (3)$$

where $\hat{\mathbf{H}}_{\mathrm{EF},k}(n) = \hat{\mathbf{F}}^*_{\mathrm{UE},k}(n)\mathbf{H}_{\mathrm{UE},k}(n)\hat{\mathbf{W}}_{\mathrm{BS},k}(n)$. If the UL and DL channels are perfectly estimated, after multiplying the postprocessor $\hat{\mathbf{U}}^*_{\mathrm{UE},k}(n)$ and the preprocessor $\hat{\mathbf{V}}_{\mathrm{BS},k}(n)$, the effective channel $\hat{\mathbf{H}}_{\mathrm{EF},k}(n)$ can completely be diagonalized to an $L_k(n)$-dimensional diagonal matrix $\hat{\mathbf{D}}_k(n)$ whose diagonal elements are singular values of the effective channel matrix $\hat{\mathbf{H}}_{\mathrm{EF},k}(n)$. Hence, the estimate in (3) is finally rewritten as

$$\tilde{\mathbf{x}}_k(n) \simeq \hat{\mathbf{D}}_k(n)\frac{P_T}{\sum_{j=1}^{K(n)} L_j(n)}\mathbf{x}_k(n) + \hat{\mathbf{R}}^*_{\mathrm{UE},k}(n)\mathbf{n}_k(n).$$

[5]We assume that the intercell interferences plus noise is complex white Gaussian, which is the worst-case assumption of the interferences and gives the lower bound of the capacity [34]. Because we consider the long-term fading of the intercell interferences, the infrequent feedback of the variance σ_k^2 from the UE to the BS is possible.

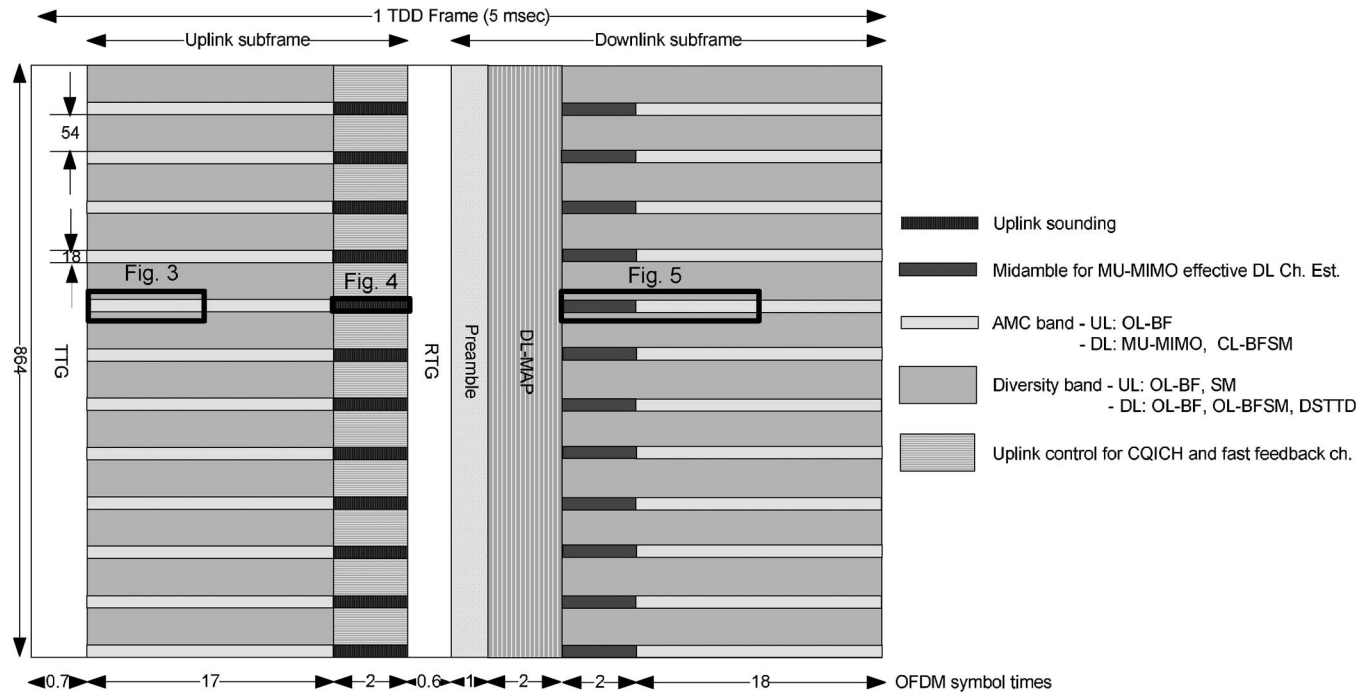

Fig. 2. TDD frame structure.

III. Time-Division Duplexing Frame Structure and Channel Estimation

In this section, the TDD frame and four types of pilot structures are introduced. We assume that the number of the BS and UEs antennas, which are denoted by N_T and N_R, is given by four and two, respectively. This antenna configuration for the practical MIMO OFDMA system is reasonable with respect to implementation issues, e.g., the spatial restriction of multiple antennas, the cost of radio frequency, system complexity, and network latency. Under the MIMO configuration, various CSI estimation methods are shown according to the designed frame and pilot structures. Estimation performance is evaluated in terms of MSE in the last part of this section.

As illustrated in Fig. 2, one TDD frame includes the UL and DL subframes, which are distinguished by the time, and the number of used subcarriers, excluding the guard subcarriers, is 864 [23], [24]. Each subframe is divided into the following two bands: 1) diversity and 2) AMC bands.[6] In diversity bands, the open-loop beamforming (OL-BF) [35], spatial multiplexing (SM) [2], OL-BFSM, and double space–time transmit diversity (DSTTD) [36] are employed. In AMC bands, the proposed MU-MIMO, OL-BF, and CL-BFSM [37] are used. Brief characteristics of the employed MIMO schemes are given as follows. OL-BF is a statistical beamforming technique that uses transmit antenna correlation. OL-BFSM is a combination of OL-BF and SM. DSTTD is a combination of space–time block coding and SM, and CL-BFSM is a combination of CL-BF and SM. The diversity and AMC bands consist of subchannels, which are the minimum unit of the resource allocation and channel coding, where each subchannel size will later be specified. The time gap between DL and UL subframes allows transition for the BS from the transmit mode to the receive mode and for the UEs from the receive mode to the transmit mode—the receive/transmit transition gap (RTG) and the transmit/receive transition gap (TTG) are the transition times between the transmit and the receive modes and between the receive and the transmit modes, respectively. At the end of the UL subframe, two subsequent OFDM symbols are used for the UL sounding and control channels. By using the UL sounding channel, where the UL training tones are transmitted to the BS, the UL CSI of the selected users for DL MU scheduling can be estimated at the BS. Feedback information can also be delivered from the UEs to the BS through the following two UL control channels: 1) the channel quality information channel (CQICH) and 2) the fast feedback channel.[7] On the DL subframe, one OFDM symbol, known as a preamble, follows the RTG for both synchronization and BS identification. Here, we assume that the DL map (DL-MAP) informing subchannel allocation and control signal is composed of two OFDM symbols. Some pilot sequence group that comprises two OFDM symbols, called midamble, is located at the beginning of the DL AMC band to estimate an effective DL CSI, which will later be explained. In the following sections, we particularly explain the design of pilot structures at the BS and UE and the estimation schemes at the UE and BS, respectively, to acquire the following channels: 1) the UL CSI of the diversity, AMC, and sounding bands; 2) the DL CSI of the diversity and AMC bands; and 3) the effective DL CSI of the AMC band.

[6]As generally assumed in [23] and [24], each subframe is divided into diversity and AMC bands to efficiently utilize the UE's different mobility characteristics. The diversity and AMC bands are partitioned by 54 and 18 subcarriers, respectively, in the frequency domain. The ratio between diversity and AMC bands can be adjusted according to the ratio between high and low mobility users.

[7]The DL SINR and the transmission modes (e.g., DSTTD, SM, and BF) are reported by using the CQICH and fast feedback channels, respectively [38].

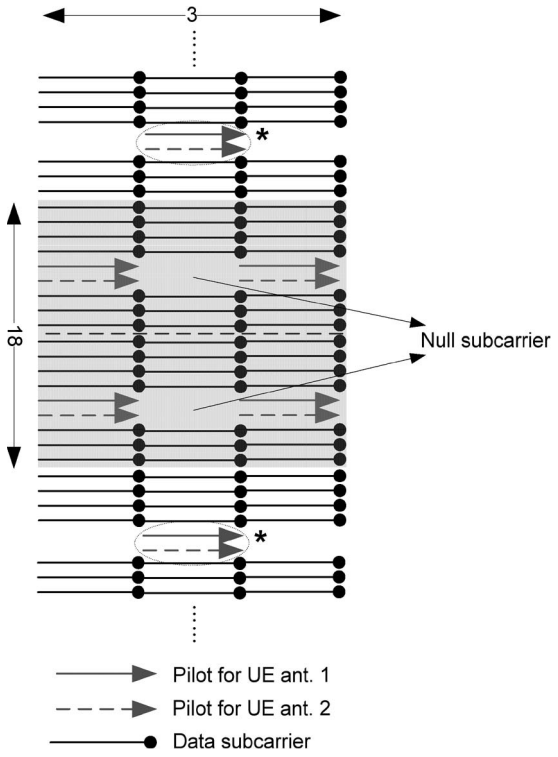

Fig. 3. UL subframe structure.

A. UL CSI of the Diversity and AMC Bands

The UL subframe structure, including UL pilots, is particularly designed to estimate the UL CSI $\mathbf{H}_{\mathrm{BS},k}(n)$ of the diversity and AMC bands for UL data recovery. Fig. 3 shows the UL subframe that contains UL subchannels composed of data, null, and pilot subcarriers, where each subchannel consists of a cluster of 18 subcarriers and 3 OFDM symbols (see Fig. 2). Here, no data and pilot subcarriers are loaded in the null subcarriers. For the OFDMA system, the estimation performance of the UL CSI is usually worse than the DL CSI. Note that the UL CSI estimation for the kth UE is performed by only using the UL pilots allocated on the kth UE's subchannels, which is contrary to the DL CSI estimation, in which common pilots over all frequency bands are used for estimation. To estimate MIMO channels in the frequency domain, pilots are assigned to the UE antennas in an orthogonal manner over the frequency domain (subcarriers). For example, if the pilots are deployed for the first antenna of the kth UE, then the second antenna of the UE does not transmit pilots on the same subcarriers used for the first antenna. In addition, to enhance the channel estimation performance, particularly at the edge of the subchannel, additional pilots (which are depicted by $*$ in Fig. 3) are allocated at the exterior of the subchannels, which are orthogonal to their neighboring subchannels, and the null subcarriers are the subcarriers left for the pilot allocation of the adjacent subchannels. This pilot design, which is denoted as a pilot-sharing scheme, enables us to have better performance for the UL CSI estimation [27]. The MMSE estimator [39] is used at the BS for the UL CSI estimation. All-one sequences are employed as the pilot sequences, because the MSE performance for MMSE-based CSI estimation does not depend on the sequence patterns [39].

B. UL CSI of the Sounding Band

Using the estimated UL CSI $\hat{\mathbf{H}}_{\mathrm{BS},k}(n)$ of the sounding band throughout the procedure described in Section III-A, it is possible for the transmitter (BS) to generate preprocessing and postprocessing matrices, i.e., $\hat{\mathbf{U}}_{\mathrm{UE},k}(n)$, $\hat{\mathbf{W}}_{\mathrm{BS},k}(n)$, and $\hat{\mathbf{V}}_{\mathrm{BS},k}(n)$, in the DL AMC band. This approach is feasible if the channel of the DL AMC band slowly enough varies to be almost identical to the CSI of the UL sounding band (note that the sounding band is located right before the DL subframe). Because the MU-MIMO scheme is applied only to the DL AMC band, the UL sounding is required only on the UL AMC bands (see Fig. 2). The specific feature of the UL sounding pilots located at the last two OFDM symbols of the UL subframe is described in Fig. 4. One sounding in the AMC band consists of a cluster that includes 18 subcarriers and two OFDM symbols. The MMSE-based channel estimator that uses a sounding signal is employed at the BS.

The remarkable characteristics of the UL sounding are the user-adaptive setup in combination with the MU-MIMO scheduler. Other features, e.g., pilot location and sequence pattern, follow the structures in [28]–[30]. Similar to other pilot sequences, the UL sounding pilots are all-one sequences and equally spaced.[8] The sounding pilots for the first and second transmitting antennas of the UE are placed at the first and second sounding OFDM symbols, respectively. Let T denote the number of users who utilize the restricted UL sounding band. Because the sounding pilots are assigned in an orthogonal manner across the frequency and time domains, the number of pilots allocated per transmit antenna of each user is given by $18/T$ for one UL sounding. Accordingly, the UL sounding structures for $T = 6, 9,$ and 18 are illustrated in Fig. 4. When $T = 6, 9,$ and 18, the number of sounding pilot subcarriers assigned for one sounding cluster per transmit antenna of each user is given by 3, 2, and 1, respectively.[9] As one of the feasible power control strategies, we perform power control for each UL sounding pilot subcarrier so that the received SINRs of the UL sounding band at the BS can be identical with all UEs [31].[10] Under the structure shown in Fig. 4, interesting observations are made as follows. As T increases, because the number of pilots per user is reduced, the MSE performance of the UL CSI estimation is degraded, resulting in more CSI uncertainty. However, the MU diversity gain increases. Therefore, a tradeoff exists between the UL CSI estimation performance and the MU diversity gain according to the number of CSI-reporting users denoted by T. In Section V, it will be shown that the optimal T is determined in terms of system throughput for various UL SINRs through the numerical results.

[8]When the MMSE estimator is applied, it is shown that the best set of pilot locations in an MSE aspect is an equally spaced pilot set [41].

[9]Note that the sounding structure can support an arbitrary T $(1 \leq T \leq 18)$ with slight modification, although the specific allocation strategy is not described in this paper.

[10]The scenario for the UL power control is described as follows. The BS estimates the channel condition from the UE that requests AMC service to the BS using sounding pilots. The BS informs the amount of increasing and decreasing power for each UE by using a DL control channel.

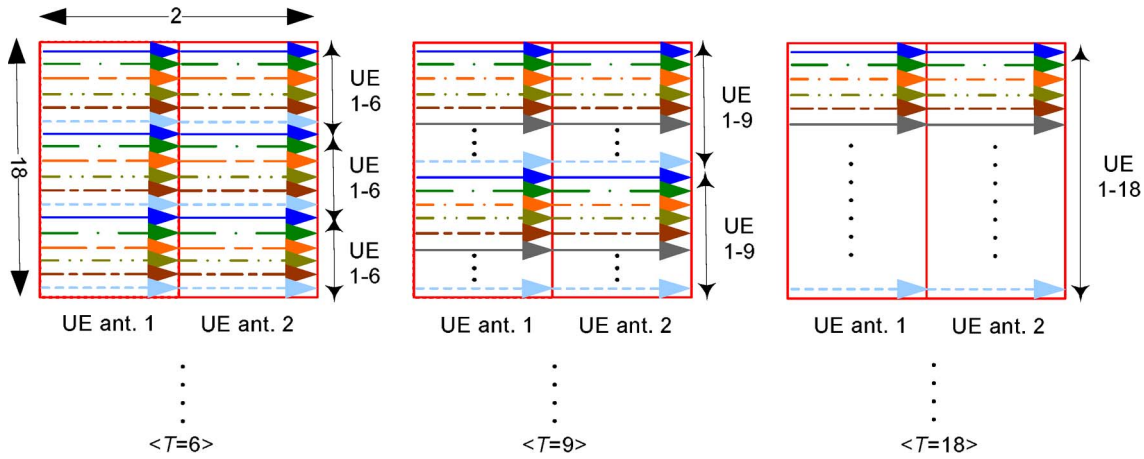

Fig. 4. UL sounding structure for the UL CSI estimation of the MU-MIMO AMC band.

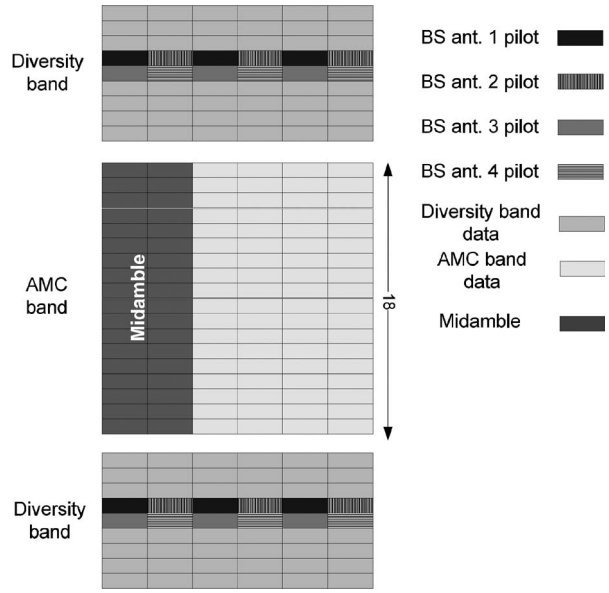

Fig. 5. DL subframe structure.

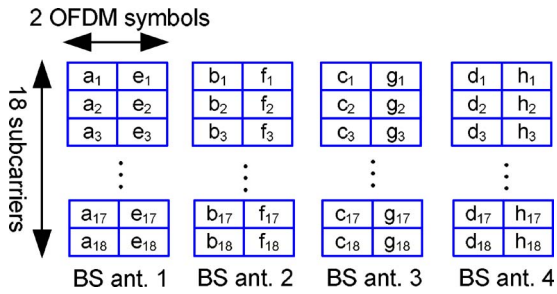

Fig. 6. Midamble structure.

C. DL CSI of Diversity and AMC Bands

Fig. 5 shows the DL subframe structure for MIMO OFDMA systems, including the DL pilot structure, where one DL diversity and AMC subchannels consist of seven equally spaced data subcarriers, six OFDM symbols, and a cluster of 18 data subcarriers and four OFDM symbols, respectively. The DL pilots are used to estimate the DL CSI $\mathbf{H}_{\mathrm{UE},k}(n)$ and then to obtain the prereceiver filter matrix $\hat{\mathbf{F}}^{*}_{\mathrm{UE},k}(n)$. DL pilots are all-one sequences and equally spaced by nine subcarriers throughout the diversity bands. The DL pilots are designed to be orthogonal across both the time and frequency domains. For example, the pilots for the channels that correspond to the first BS antenna are placed at an odd time and even frequency subcarriers in each diversity subchannel, whereas the null subcarriers are assigned for the other antennas of BS. Similarly, orthogonal pilots are allocated to the subcarriers of other transmit antennas. The DL CSI of both diversity and AMC bands is estimated by using only the pilots on the diversity band. That is, no DL pilot is allocated at the DL AMC bands to avoid additional overhead for training, which leads to reduced spectral efficiency. However, because the DL pilots in the diversity bands can be received by all UEs, including both AMC and diversity users, each user can estimate the overall DL CSI by using the pilots in the diversity bands. This design may yield performance degradation on the estimation for DL CSI. Compared with the case with extra pilots for the AMC band, however, the normalized MSE increase is negligible, as shown in the computer simulation described in Section III-E.

D. Effective DL CSI of the AMC Band

In this section, we describe the midamble structure shown in Figs. 5 and 6 and propose an effective DL CSI estimation scheme, which allows for the UEs to obtain their MU-MIMO postprocessing matrix. The estimated MU-MIMO postprocessing matrix $\hat{\mathbf{U}}^{*}_{\mathrm{UE},k}(n)$ is the left singular matrix of the effective DL CSI $\hat{\mathbf{H}}_{\mathrm{EF},k}(n)$ in (3). Because the left singular vector of $\hat{\mathbf{H}}_{\mathrm{EF},k}(n)$ is the same as in $\hat{\mathbf{H}}_{\mathrm{EF},k}(n)\hat{\mathbf{V}}_{\mathrm{BS},k}(n)$, which is equivalent to $\hat{\mathbf{F}}^{*}_{\mathrm{UE},k}(n)\mathbf{H}_{\mathrm{UE},k}(n)\hat{\mathbf{T}}_{\mathrm{BS},k}(n)$, the estimation for $\mathbf{H}_{\mathrm{UE},k}(n)\hat{\mathbf{T}}_{\mathrm{BS},k}(n)$ is also required to generate the postprocessing matrices at the UE. Noting that $\hat{\mathbf{F}}^{*}_{\mathrm{UE},k}(n)$ is obtained from the procedure shown in Section III-C, to obtain $\mathbf{H}_{\mathrm{UE},k}(n)\hat{\mathbf{T}}_{\mathrm{BS},k}(n)$ for the kth user, we can consider the following two communication scenarios: 1) the feedforward scheme and 2) the estimation-and-interpolation scheme. In the former strategy, the BS forwards the preprocessing matrix by using a signaling channel. In the latter strategy, the UEs estimate the effective DL CSI by using DL pilots that were

described in the previous section. However, the aforementioned scenarios have problems. For the feedforward scheme, because the size of the complex preprocessing matrix $\hat{\mathbf{T}}_{\mathrm{BS},k}(n)$ is $N_T \times L_k(n)$, the BS needs to forward at least $2N_T \sum_{k=1}^{K(n)} L_k(n)$ real values per subcarrier, where $K(n) \in \{1, \cdots, N_T\}$ is the number of supported users at the nth subcarrier. Hence, the feedforward information significantly reduces the DL throughput, resulting in an inefficient system. On the other hand, for the estimation-and-interpolation scheme, it is difficult to interpolate the effective DL CSI estimated by DL pilots due to the discontinuity of the preprocessing matrices among the consecutive subcarriers. This discontinuity comes from the fact that the preprocessing matrix contains the IUI suppression matrix generated from nonunique nullspaces.

Alternatively, we propose a midamble-based estimation method for the estimation of effective DL CSI. Each midamble band consists of a cluster with 18 subcarriers and two OFDM symbols. The midamble sequences are particularly designed by

$$\begin{bmatrix} a_n & b_n & c_n & d_n \\ e_n & f_n & g_n & h_n \end{bmatrix}^T = \sum_{k=1}^{K(n)} \hat{\mathbf{T}}_{\mathrm{BS},k}(n)\mathbf{P}_{k,L_k(n)}$$

where $\mathbf{P}_{k,L_k(n)}$ is the known symbol made from $L_k(n)$ rows of the N_R-dimensional identity matrix, i.e., $\mathbf{P}_{k,1} = [1\ 0]$ or $[0\ 1]$ and $\mathbf{P}_{k,2} = \begin{bmatrix} 1 & 0 \\ 0 & 1 \end{bmatrix}$, and is located at one cluster, as shown in Fig. 6. Note that two OFDM symbols are used to generate $\mathbf{P}_{k,L_k(n)}$, whose ith column corresponds to the ith symbol. The BS needs to simultaneously transmit the midamble to support users (i.e., UEs) as small as possible to reduce the IUI so that UEs can reliably estimate the effective CSI. Now, we mainly focus on the case where the number of supported users at each subcarrier is two, i.e., $K(n) = 2$ (the other cases can be shown with a slight modification). Then, according to the number $L_k(n)$ of streams at each user, two types of midambles are designed as follows.

- *Orthogonal midamble*
  - $\mathbf{P}_{1,1} = [1\ 0]$, and $\mathbf{P}_{2,1} = [0\ 1]$.
  - $\mathbf{P}_{1,1} = [0\ 1]$, and $\mathbf{P}_{2,1} = [1\ 0]$.
- *Superimposed midamble*
  - $\mathbf{P}_{1,2} = \begin{bmatrix} 1 & 0 \\ 0 & 1 \end{bmatrix}$, and $\mathbf{P}_{2,1} = [1\ 0]$.
  - $\mathbf{P}_{1,2} = \begin{bmatrix} 1 & 0 \\ 0 & 1 \end{bmatrix}$, and $\mathbf{P}_{2,1} = [0\ 1]$.
  - $\mathbf{P}_{1,1} = [1\ 0]$, and $\mathbf{P}_{2,2} = \begin{bmatrix} 1 & 0 \\ 0 & 1 \end{bmatrix}$.
  - $\mathbf{P}_{1,1} = [0\ 1]$, and $\mathbf{P}_{2,2} = \begin{bmatrix} 1 & 0 \\ 0 & 1 \end{bmatrix}$.
  - $\mathbf{P}_{1,2} = \mathbf{P}_{2,2} = \begin{bmatrix} 1 & 0 \\ 0 & 1 \end{bmatrix}$.

For example, when the BS supports two users who transmit one spatial stream for the nth subcarrier, i.e., $[L_1(n)\ L_2(n)] = [1\ 1]$, if $\mathbf{P}_{1,1} = [1\ 0]$ for one user, then $\mathbf{P}_{2,1} = [0\ 1]$ for the other user. If the channel is assumed to be static within two consecutive OFDM symbols at the midamble band, then the received signal $\mathbf{Y}_k(n) = [\mathbf{y}_k(n,1)\ \mathbf{y}_k(n,2)] \in \mathbb{C}^{N_R \times N_R}$ of the kth user can be represented as

$$\begin{aligned}
&[\mathbf{y}_k(n,1)\ \mathbf{y}_k(n,2)] \\
&\quad = \mathbf{H}_{\mathrm{UE},k}(n) \sum_{j=1}^{K(n)} \hat{\mathbf{T}}_{\mathrm{BS},j}(n)\mathbf{P}_{j,L_j(n)} + \mathbf{N}_k(n) \\
&\quad = \mathbf{H}_{\mathrm{UE},k}(n)\hat{\mathbf{T}}_{\mathrm{BS},k}(n)\mathbf{P}_{k,L_k(n)} \\
&\qquad + \mathbf{H}_{\mathrm{UE},k}(n) \sum_{j=1, j\neq k}^{K(n)} \hat{\mathbf{T}}_{\mathrm{BS},j}(n)\mathbf{P}_{j,L_j(n)} + \mathbf{N}_k(n) \qquad (4)
\end{aligned}$$

where $\mathbf{y}_k(n,i)$ is the ith column vector of $\mathbf{Y}_k(n)$ for $i = 1, 2$, and $\mathbf{N}_k(n) \in \mathbb{C}^{N_R \times N_R}$ is the time-extended matrix representation of $\mathbf{n}_k(n)$ in (2). Note that, if the UL CSI estimation in Section III-A is perfect, then the IUIs, which are the second term in (4), are completely canceled out. When a least squares estimator for $\mathbf{H}_{\mathrm{UE},k}(n)\hat{\mathbf{T}}_{\mathrm{BS},k}(n)$ is used here, the estimate is simply given by

$$\widehat{\mathbf{H}_{\mathrm{UE},k}(n)\hat{\mathbf{T}}_{\mathrm{BS},k}}(n) = \mathbf{Y}_k(n).$$

Consequently, the estimated left singular vector $\hat{\mathbf{U}}^*_{\mathrm{UE},k}(n)$ of the effective DL CSI can be taken into account as the left singular vector of the matrix $\hat{\mathbf{F}}^*_{\mathrm{UE},k}(n)\mathbf{Y}_k(n)$. In particular, when $\mathbf{P}_{k,1} = [1\ 0]$ or $[0\ 1]$, i.e., the orthogonal midamble is used, $\hat{\mathbf{U}}^*_{\mathrm{UE},k}(n)$ is estimated from the left singular vector of $\hat{\mathbf{F}}^*_{\mathrm{UE},k}(n)\mathbf{y}_k(n,1)$ or $\hat{\mathbf{F}}^*_{\mathrm{UE},k}(n)\mathbf{y}_k(n,2)$, respectively. On the other hand, when $\mathbf{P}_{k,2} = \begin{bmatrix} 1 & 0 \\ 0 & 1 \end{bmatrix}$, $\hat{\mathbf{U}}^H_{\mathrm{UE},k}(n)$ is estimated from the left singular vector of $\mathbf{Y}_k(n)$, because there is no combining of the received signal, and $\hat{\mathbf{F}}^*_{\mathrm{UE},k}(n)$ is then represented as the identity matrix. Therefore, each UE needs only 2 b of feedforward information per subchannel to distinguish three types of midamble sequences [1 0], [0 1], and $\begin{bmatrix} 1 & 0 \\ 0 & 1 \end{bmatrix}$. Note that this feedforward quantity is substantially lower than the quantity required for other signaling methods in the feedforward and the estimation-and-interpolation schemes.

E. MSE Performance

In this section, we evaluate the normalized MSE[11] of various CSI according to SINR values. The MSE results for the UL CSI of the diversity and AMC bands, the UL CSI of the sounding band, the DL CSI of the diversity and AMC bands, and the effective DL CSI of the AMC bands are illustrated in Figs. 7–10, respectively.

In Fig. 7, it is shown that the normalized MSE performance at the UL diversity bands degrades as the velocity increases. It is also found that the MSE performance of UL AMC bands is slightly worse than the UL diversity bands when the velocity

[11]The normalized MSE is used as a performance measure of the estimator, because it reflects both the bias and the variance of an estimate and is defined as $E[\|\hat{\mathbf{H}} - \mathbf{H}\|^2/\|\mathbf{H}\|^2]$, where $\mathbf{H}$ and $\hat{\mathbf{H}}$ are the actual and estimated channels, respectively.

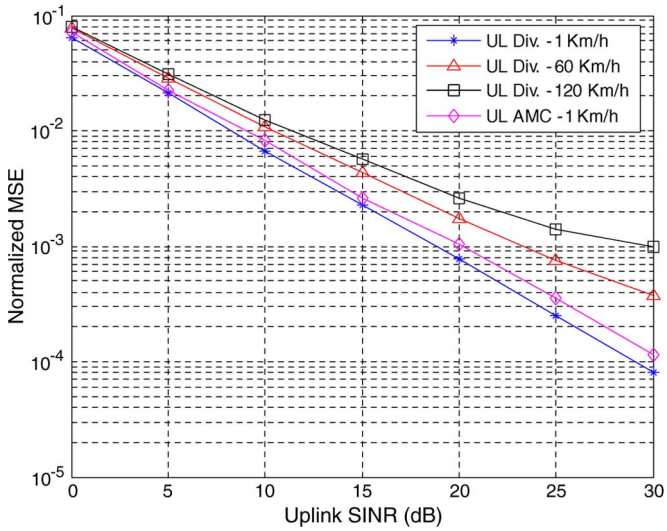

Fig. 7. Normalized MSE performance for the UL CSI estimation.

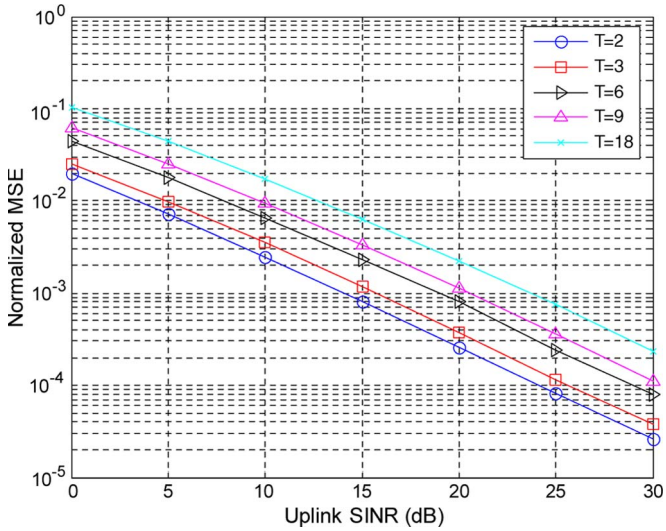

Fig. 8. Normalized MSE performance for the UL CSI estimation of the sounding band.

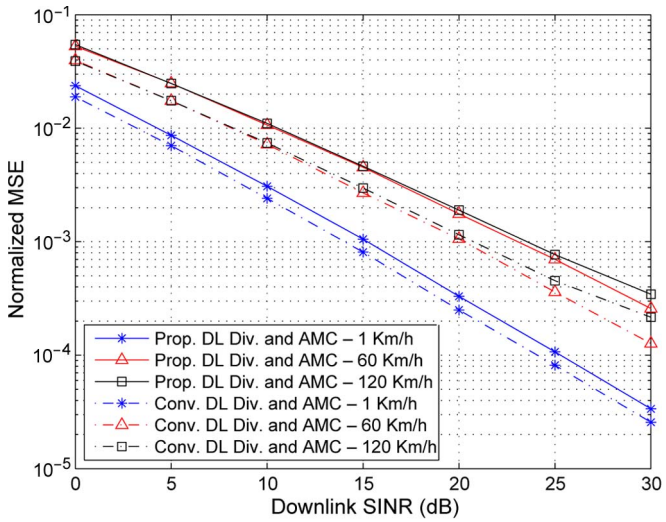

Fig. 9. Normalized MSE performance for the DL CSI estimation of the diversity and AMC bands when $T = 6$.

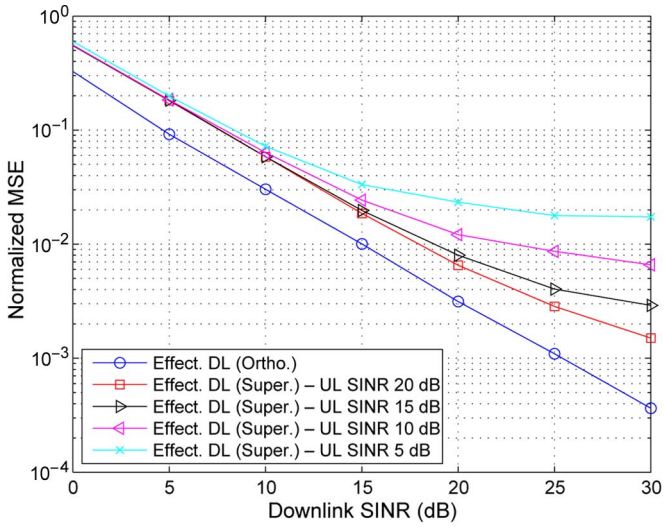

Fig. 10. Normalized MSE performance for the effective DL CSI estimation of the AMC band when $T = 6$ and $K(n) = 2$.

is 1 km/h due to the relatively small number of pilots. The UL diversity bands can utilize more pilots to estimate their UL CSI than the UL AMC bands, because the pilots within one subchannel are sparsely allocated across the frequency domain in the UL diversity bands.

In Fig. 8, assuming that the velocity of UEs is 1 km/h, it is shown that the MSE performance degrades as T increases, because the number of allocated pilots per user is reduced. For example, when $T = 6$, a 3-dB increment of the UL SINR is required to obtain the same normalized MSE as when $T = 3$.

The normalized MSE for the DL CSI estimation of the diversity and AMC bands is also shown in Fig. 9. It is shown that the MSE performance degrades as the velocity increases, as in the case of UL CSI estimation. Because the DL CSI is estimated by not using the pilots in the DL AMC bands but in the DL diversity bands ("Prop. DL Div. and AMC"), the MSE performance becomes worse compared to the case when the pilots are employed in both bands ("Conv. DL Div. and AMC"). The SINR loss for the MSE performance is, however, shown within 1.5 dB for each velocity.

Fig. 10 shows a normalized MSE for the effective DL CSI estimation of AMC bands when $T = 6$ and $K(n) = 2$. Note that MSE performance is affected by the UL SINR for sounding bands, because the UL CSI estimation is related to the IUI. If the orthogonal midamble is used, i.e., $[L_1(n)\ L_2(n)] = [1\ 1]$, then the MSE performance becomes the best and is irrelevant to the UL SINR, because the IUI does not occur. On the other hand, when $[L_1(n)\ L_2(n)] = [2\ 2]$, the superimposed midamble is used, where the MSE performance depends on the UL SINR and the corresponding IUIs. It is shown that, when the superimposed midamble is used at a low UL SINR, the MSE performance does not improve much, even at a high DL SINR. Then, a MSE error floor is observed.[12]

[12]Although not shown in this paper, when $[L_1(n)\ L_2(n)] = [1\ 2]$ or $[2\ 1]$, the MSE curve is located in between two cases by using the orthogonal and the superimposed midambles with four spatial streams (i.e., $[L_1(n)\ L_2(n)] = [2\ 2]$).

IV. Practical and Simplified Scheduling Algorithm

In this section, we propose a practical and simple algorithm for the resource allocation (i.e., scheduling) of the MU-MIMO OFDMA system. The scheduling includes the following two procedures: 1) the selection of supported users and 2) the assignment of their spatial modes, i.e., the number of data streams.

A. Problem Formulation and the EX-Search Algorithm

We first define the users-and-modes vector $\mathbf{\Omega}$, where $\mathbf{\Omega} = [\mathbf{\Omega}(1) \ \cdots \ \mathbf{\Omega}(B)]$, B denotes the number of subcarriers occupied by AMC bands, and $\mathbf{\Omega}(n) = [L_1(n) \ \cdots \ L_T(n)]$ represents the number of spatial streams allocated to T users for the nth subcarrier. We now determine the vector $\mathbf{\Omega}$ in terms of maximizing the throughput, which can be computed by using the estimated UL channels $\{\hat{H}_{\mathrm{BS},k}(n)\}$. By substituting $\hat{\mathbf{U}}^*_{\mathrm{BS},k}(n)$, $\hat{\mathbf{F}}^*_{\mathrm{BS},k}(n)$, and $\hat{\mathbf{H}}_{\mathrm{BS},k}(n)$ to $\hat{\mathbf{U}}^*_{\mathrm{UE},k}(n)$, $\hat{\mathbf{F}}^*_{\mathrm{UE},k}(n)$, and $\mathbf{H}_{\mathrm{UE},k}(n)$ in (3), respectively, and using the estimated DL received signal model, we show an information-theoretic users-and-modes selection criterion that maximizes the estimated weighted-sum achievable rates as follows:

$$\max_{\mathbf{\Omega}} \sum_{n=1}^{B} \sum_{k=1}^{T} \mu_k R_k(n) \tag{5a}$$

$$\text{subject to } 0 \le L_k(n) \le N_R \text{ and } \sum_{k=1}^{T} L_k(n) \le N_T \tag{5b}$$

where

$$R_k(n) = \log\det\left(\mathbf{I}_{L_k(n)} + \frac{P_T}{\sigma_k^2 \sum_{j=1}^{T} L_j(n)} \times \hat{\mathbf{D}}_{\mathrm{BS},k}(n)\hat{\mathbf{D}}^*_{\mathrm{BS},k}(n)\right)$$

$$\hat{\mathbf{D}}_{\mathrm{BS},k}(n) = \hat{\mathbf{U}}^*_{\mathrm{BS},k}(n)\hat{\mathbf{F}}^*_{\mathrm{BS},k}(n)\hat{\mathbf{H}}_{\mathrm{BS},k}(n) \times \hat{\mathbf{W}}_{\mathrm{BS},k}(n)\hat{\mathbf{V}}_{\mathrm{BS},k}(n) \tag{6}$$

and the constraint (5b) is a necessary and sufficient condition for eliminating cochannel interference (CCI) in the spatial domain [10]. Here, the weighting factor μ_k is used for fairness among the users. For the proportional fairness (PF) scheduling, μ_k is given by the inverse of the time-averaged past throughput [15] and is updated as follows:

$$\frac{1}{\mu_k} = \left(1 - \frac{1}{t_w}\right)\frac{1}{\bar{\mu}_k} + \frac{R_k(n)}{t_w}, \quad k \in \mathcal{S}$$

$$\frac{1}{\mu_k} = \left(1 - \frac{1}{t_w}\right)\frac{1}{\bar{\mu}_k}, \quad k \notin \mathcal{S}$$

where t_w is the size of the window that is averaged out over time, $\bar{\mu}_k$ is the kth user's weighting factor at the previous scheduling time, and $\mathcal{S}$ is an index set for the nonzero elements of $\mathbf{\Omega}(n)$. On the one hand, when $\mu_1 = \cdots = \mu_T$, the scheduler becomes the maximum rate scheduler, which maximizes the sum achievable rates without considering fairness.

In practice, because $\mathbf{\Omega}$ is independently determined for each channel coding block, which is the congregation of some subcarriers, the aforementioned users-and-modes selection in (5) may not directly be applied to practical systems. We thus slightly modify the selection criterion by applying the following design rules. Within one channel coding block, suppose that $\mathbf{\Omega}(n)$ is the same for all n, i.e., $\mathbf{\Omega}_g = \mathbf{\Omega}(1 + M(g-1)) = \cdots = \mathbf{\Omega}(Mg)$ for $g = 1, \cdots, G$, where $G = B/M$, G is the number of channel coding blocks, and M denotes the number of subcarriers in one channel coding block. The modulation and coding scheme (MCS) is then selected as the largest among the spectral efficiencies, which guarantee the target frame error rate (FER) for each subcarrier in one coding block.[13] Accordingly, with modification, the users-and-modes selection criterion in (5) can be rewritten as

$$\max_{\mathbf{\Omega}} \sum_{g=1}^{G} \sum_{k=1}^{T} \sum_{i=1}^{L_{k,g}} \mu_k M \min_{m \in \{1,\cdots,M\}} \mathrm{MCS}(\mathrm{SINR}_{m,g,i}) \tag{7a}$$

$$\text{subject to } 0 \le L_{k,g} \le N_R \text{ and } \sum_{k=1}^{T} L_{k,g} \le N_T \tag{7b}$$

where $L_{k,g} = L_k(m + M(g-1))$ for $m = 1, \cdots, M$, $\mathrm{SINR}_{m,g,i} = P_T \hat{d}^2_{m,g,i}/(\sigma_k^2 \sum_{j=1}^{T} L_{j,g})$, $\hat{d}_{m,g,i}$ is the ith diagonal element of $\hat{\mathbf{D}}_{\mathrm{BS},k}(m + M(g-1))$ in (6), and $\min_m \mathrm{MCS}(\mathrm{SINR}_{m,g,i})$ denotes the minimum among M MCS values in the gth coding block. As aforementioned, the optimization of (5) and (7), conducted by the EX search, requires a great amount of excessive computational complexity when the total number of users increases.[14] To reduce the computational load, a suboptimal algorithm is introduced in the following section.

B. TR-Search Algorithm

A suboptimal TR-search algorithm is proposed based on the stack search [32] with unit stack size. The algorithm is a general version of the previous work in [33] so that it can include the case when the number T of total users is greater than or equal to the number N_T of transmit antennas. Because the optimization problem in (7) can independently be solved for each channel coding block, the TR-search algorithm is described only for the gth channel coding block. Denoting the kth node (element) in the lth stack (stage) at the gth channel coding block by $\Omega_g^{l,k}$, the proposed TR-search algorithm is described in Algorithm 1. Note that, based on this algorithm, the configuration $\Omega_g^{l,\max}$ can be chosen by locally maximizing the sum achievable rates at each stage.

[13] We design the MCS-level selection method without considering the hybrid automatic repeat request (HARQ), which remains for future work.

[14] A combinational search of the EX-search algorithm in (5) is given by $G\sum_{k=1}^{N_T} {}_T\mathrm{C}_k J_k$, where ${}_T\mathrm{C}_k = T!/(k!(T-k)!)$, $x! = x(x-1)\cdots 1$, and J_k is the number of possible spatial modes for k users under (7b). More details will be analyzed in Section IV-C.

TABLE I
NUMBER OF OPERATIONS (MULTIPLICATION AND ADDITION) REQUIRED FOR BASIC COMPUTATION (FLOPS)

Selected users	Operations	Computational complexity
$K(n)=1$	Singular values and left singular vector of $\hat{\mathbf{H}}_{\mathrm{BS},k}(n)$	$24N_TN_R^2+48N_R^3$
	Multiplication: $\hat{\mathbf{F}}^*_{\mathrm{BS},k}(n)\hat{\mathbf{H}}_{\mathrm{BS},k}(n)$ in (6)	$6N_TN_R^2$
$K(n)\geq 2$	Nulling matrix: $\hat{\mathbf{W}}_{\mathrm{BS},k}(n)$ in (1)	$24N_T^2\sum_{\substack{j=1\\j\neq k}}^{K(n)}L_j(n)+48N_T\Big(\sum_{\substack{j=1\\j\neq k}}^{K(n)}L_j(n)\Big)^2$
	Multiplication: $\hat{\mathbf{F}}^*_{\mathrm{BS},k}(n)\hat{\mathbf{H}}_{\mathrm{BS},k}(n)\hat{\mathbf{W}}_{\mathrm{BS},k}(n)$ in (6)	$6L_k(n)N_T\Big(N_T-\sum_{\substack{j=1\\j\neq k}}^{K(n)}L_j(n)\Big)$
	Singular values: $\hat{\mathbf{D}}_{\mathrm{BS},k}(n)$ in (6)	$24L_k^2(n)\Big(N_T-\sum_{\substack{j=1\\j\neq k}}^{K(n)}L_j(n)\Big)-8L_k^3(n)$

TABLE II
NUMBER OF OPERATIONS (MULTIPLICATION AND ADDITION) REQUIRED FOR THE USER-AND-SPATIAL MODE SELECTION (FLOPS)

Selection methods	Number of operations ($L_k(n)=1$)
Exhaustive (EX)-search	$\mathcal{F}(T,N_T,N_R)>T(24N_TN_R^2+48N_R^3+6N_TN_R^2)$ $+\sum_{K=2}^{\min(T,N_T)}[{}_{\mathrm{T}}\mathrm{C}_{\mathrm{K}}(48K^3N_T+K^2(24N_T^2-102N_T-24)+K(-18N_T^2+78N_T+16)]$
Trimming (TR)-search	$\mathcal{F}(T,N_T,N_R)\simeq T(60N_T^2+30N_R^2N_T+132N_T+48N_R^3-64)-60N_T^2-132N_T+64$ $+\sum_{K=3}^{\min(T,N_T)}[K^3(48TN_T-48N_T)+K^2(24TN_T^2-24N_T^2-102TN_T+48N_T-24T+24)$ $+K(-18TN_T^2+24N_T^2+78TN_T+84N_T+16T-72)-84N_T+48]$

Algorithm 1: **TR-search algorithm**.

Define

$$C\left(\mathbf{\Omega}_g^{l,k}\right)=\sum_{k=1}^{T}\sum_{i=1}^{L_{k,g}}\mu_kM\min_{m\in\{1,\cdots,M\}}\mathrm{MCS}(\mathrm{SINR}_{m,g,i})$$

in (7a).

for $g=1$ to G **do**
for $k=1$ to T **do**
$L_{k,g}=0$
end for
$C_{\max}=0$
while $\sum_{k=1}^{T}L_{k,g}<N_T$ **do**
for $k=1$ to T **do**
if $L_{k,g}<N_R$ **then**
$\beta_k=C([L_{1,g}\ \cdots\ L_{k,g}+1\ \cdots\ L_{T,g}])$
else
$\beta_k=-1$
end if
$C_0=\max_k\beta_k$
if $C_0\leq C_{\max}$ **then**
break
end if
$C_{\max}=C_0$
$\mathbf{\Omega}_g^{l,\max}=[L_{1,g}\ \cdots\ L_{p,g}+1\ \cdots\ L_{T,g}]$
end for
end while
end for

C. Analysis of Computational Complexity

In this section, the computational complexities for both the EX and TR searches are analyzed. The overall complexities are G times the complexities for selecting Ω in the gth channel coding block. The basic computation complexities are summarized in Table I based on the Golub–Reinsch singular value decomposition algorithm [42]. The number of floating operations (flops; multiplications plus additions) involved in selecting users and modes is denoted by $\mathcal{F}(T,N_T,N_R)$, with given parameters of T, N_T, and N_R, and is shown in Table II. For simplicity, the optimal number of the spatial streams is assumed to be one. After some manipulation, the computational complexity order of the EX and TR searches is derived by $\mathcal{O}(T^{N_T})$ and $\mathcal{O}(T)$, respectively.[15] It is obvious that the complexity of the EX-search method is much higher than the TR-search method, particularly when the number of users increases. Fig. 11 illustrates the number of flops for the EX and TR searches as a function

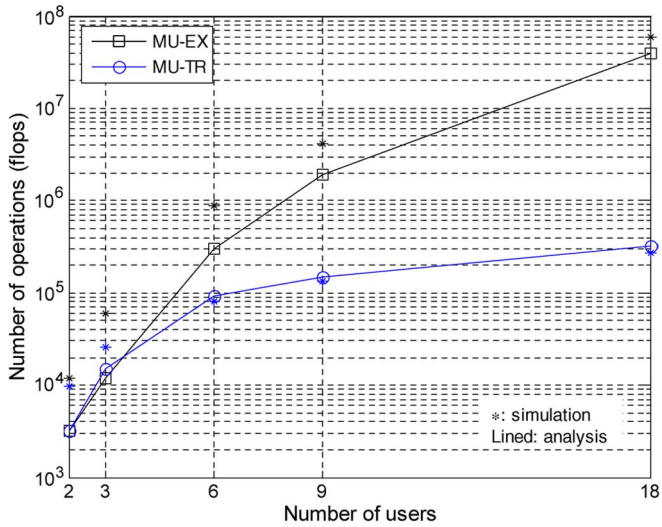

Fig. 11. Number of operations versus the number of users when $N_T=4$ and $N_R=2$.

[15] $f(x)=\mathcal{O}(g(x))$ means that positive constants C and c exist such that $f(x)\leq Cg(x)$ for all $x>c$.

TABLE III
SYSTEM PARAMETERS [23]

Parameters	Valuses	Parameters	Valuses
# of antennas $\{N_T,N_R\}$	$\{4,2\}$	Subcarrier spacing	9.7656 KHz
Carrier frequency	2.3 GHz	Symbol time	102.4 μsec
Bandwidth	8.75 MHz	CP time	12.8 μsec
Sampling frequency	10 MHz	Frame length	5 msec
DFT size	1024	OFDM symbol per frame	42
Used subcarrier	864	TTG/RTG time	87.2/74.4 μsec

TABLE IV
MULTICELL ENVIRONMENTS [43]

Parameter	Values	Parameter	Values
BS power+antenna gain	$43+4$ dBm	Propagation model	Cost 231 Urban
UE power	23 dBm	Path loss exponent	3.5
Noise level	-94 dBm	Shadowing STD	8.9 dB
Radius of cell	1000 m	BS correlation	0.5
Inter-cell	18 (2nd-tier)	Min. separation (d_0)	35 m
Tx antenna pattern	Omni-direction	Max. achievable SINR	20 dB

of the number of users. It is shown that the numerical and analytical results match well as the number of users increases. The numerical results are evaluated from the sum achievable rates shown in the next section.

V. THROUGHPUT EVALUATION

In this section, to demonstrate the advantage of the proposed MU-MIMO OFDMA system over the existing MIMO OFDMA system, i.e., CL-BFSM, we perform a system-level simulation that evaluates the system throughput. In particular, the sum achievable rates in the DL AMC bands are examined according to various UL SNRs and the number T of UL sounding users. The overall average cell throughput is also evaluated under four different bands—UL diversity, DL diversity, UL AMC, and DL AMC bands—by considering the overhead of the TTG, RTG, preamble, DL-MAP,[16] and pilots in Fig. 2.

A. Simulation Environments

We describe our basic assumptions, system parameters, and multicell environments as follows.

- *Basic assumptions*. The PF scheduler [15] is employed. Initial synchronization, including the frame, timing, and carrier frequency, is perfectly executed. The power of the pilot subcarriers at both the UL and the DL is boosted by 2.5 dB compared to the data subcarriers [31]. The velocity of AMC users is 1 km/h, whereas the velocity of diversity users is 1, 60, or 120 km/h, and the target FER is given by 10^{-2}.
- *System parameters*. $N_T=4$, and $N_R=2$. The basic OFDM parameters, such as carrier frequency, bandwidth, and DFT size, are the same as the parameters of the mobile WiMAX standards [23], [24], and more specific system parameters are listed in Table III.
- *Multicell environments*. The simulation methodology of the Third-Generation Partnership Project 2 (3GPP2) is employed to construct a multicell environment [43]. A cell is formed as a hexagon whose radius is 1000 m. The cell is piled up in the nearest outer 18 cells. The users are randomly distributed in a uniform manner. The propagation model follows the COST 231 Urban model, which is also known as the personal communication system extension to the Hata model [44]. More specific system parameters are listed in Table IV.

The considered AMC parameters are listed in Table V. The convolutional turbo code (CTC) is used as our coding scheme, and the eight MCS levels, which include the smallest and largest code rates among 32 levels, are selected from the CTC of IEEE 802.16e [31]. To support the boundary users at each cell, 1/12, 1/8, and 1/4 code rates of CTC are obtained by repetition. Input information bits and spectral efficiency denote the total number of transmitting bits per spatial stream for one AMC band and the number of bits per channel use (pcu), respectively.

B. Sum Achievable Rates in DL AMC Bands

Based on the frame structures and simulation environments, we are ready to run the system-level simulation, which shows the sum achievable rates (bits per subcarrier) of the proposed MU-MIMO and conventional MIMO OFDMA systems in the

[16]We assume that each UE can perfectly decode the DL-MAP due to the strongest channel coding scheme, such as the quadrature phase-shift keying of code rate 1/12 in the IEEE Std. 802.16 [24], [31] and 3GPP standards [43]. Any orthogonal mapping rule between the BS antennas and the DL-MAP can be possible, although the specific mapping rule is not described in this paper.

TABLE V
AMC PARAMETERS [31]

Modulation	CTC coding rate	Input information bits	Spectral efficiency (bits pcu)
QPSK	1/12	54	1/6
QPSK	1/8	81	1/4
QPSK	1/4	162	1/2
QPSK	1/2	324	1
16QAM	1/2	648	2
16QAM	3/4	972	3
64QAM	2/3	1296	4
64QAM	5/6	1620	5

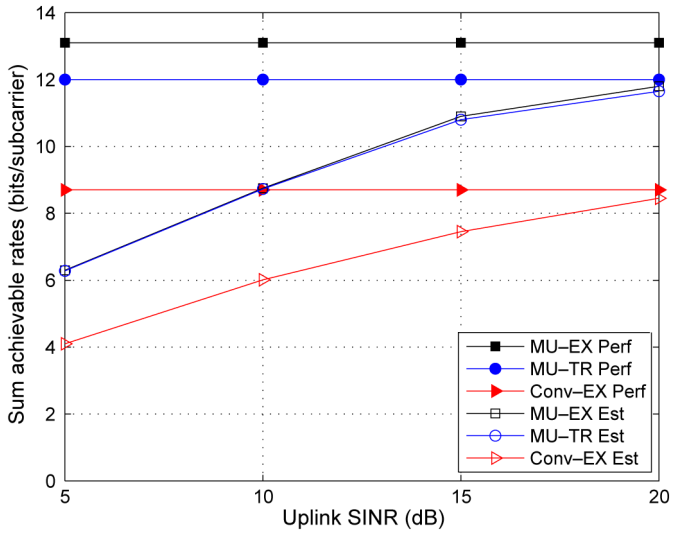

Fig. 12. Sum achievable rates in the DL AMC bands versus the UL SINR in the UL sounding band when $T = 6$ and the DL SINR is higher than 10 dB in the DL AMC bands.

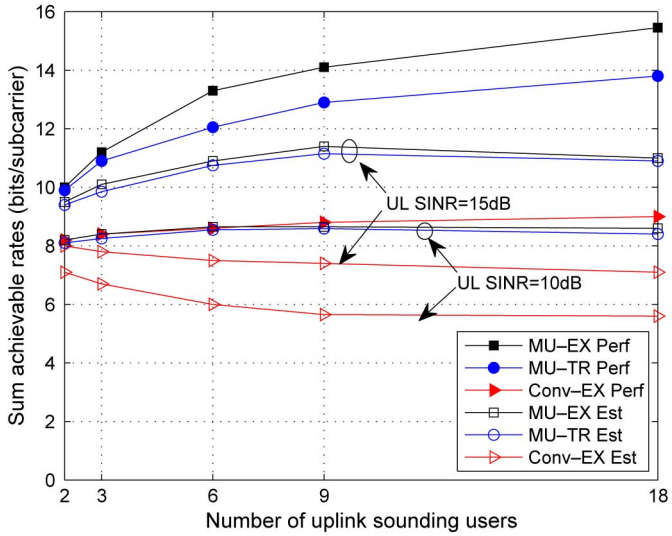

Fig. 13. Sum achievable rates in the DL AMC bands versus the number T of UL sounding users, where the DL SINR is higher than 10 dB, and the UL SINR in the UL sounding band is given by 10 and 15 dB in the DL AMC bands.

DL AMC bands. The simulation is simultaneously performed with the MU scheduling after running the multicell simulation. The proposed MU-MIMO and CL-BFSM [37] schemes[17] are employed for the MU-MIMO and MIMO systems, respectively, in the DL AMC bands.

Fig. 12 shows the sum achievable rates in the DL AMC bands versus the UL SINR in the UL sounding band. It is assumed that the number of DL AMC users is 6, where such users with a SINR of higher than 10 dB are randomly selected. As an upper bound on the performance, for the case when the UL CSI of the sounding band, DL CSI, and effective DL CSI are perfectly estimated, the maximum sum achievable rates are given by 13.1, 12, and 8.7 b/subcarrier in the following three systems, respectively: 1) MU-MIMO systems with the EX search and perfect estimation (MU-EX-Perf); 2) MU-MIMO systems with the TR search and perfect estimation (MU-TR-Perf); and 3) conventional MIMO systems with the EX search and perfect estimation (Conv-EX-Perf). The sum achievable rates of the proposed MU-TR-Perf are comparable with the optimal MU-EX-Perf within approximately 8.5% performance loss. We now consider the cases with CSI estimation error, which leads to reduced sum achievable rates. In practice, as the UL SINR increases, the sum achievable rates of the MU-MIMO system increase due to the reduced IUI. In addition, some interesting observation is shown in Fig. 12 and is described as follows. The MU-MIMO systems with the TR search and estimation error (MU-TR-Est) show the nearly same sum achievable rates as in the MU-MIMO systems with the EX search and estimation error (MU-EX-Est). For the MU-TR-Est, we obtain a sum achievable rate gain up to 38% under the UL SINRs from 5 dB to 20 dB compared with the conventional MIMO systems with the EX search and estimation error (Conv-EX-Est).

Fig. 13 shows the sum achievable rates in the DL AMC bands versus the number T of UL sounding users who report their own CSI. The sum achievable rates of MU-EX-Perf, MU-TR-Perf, and Conv-EX-Perf tend to grow as T increases because of the MU diversity gain. However, the sum achievable rates of MU-EX-Est, MU-TR-Est, and Conv-EX-Est do not always monotonically increase with respect to T. This is because the number of sounding pilots per user varies according to T, and the CSI uncertainty is changed. As T increases, the MU

[17]In particular, the CL-BFSM is identical to the proposed MU-MIMO, assuming that a UE is always supported for each AMC band.

TABLE VI
LINK-LEVEL LOOKUP TABLE FOR THE UL AMC: SINR (IN DECIBELS; TRANSMISSION MODE)

bits/subcarrier	1/6	1/4	1/2	1	2	3	4	5
1 Km/h	-3.1 (BF)	-2.34 (BF)	0.50 (BF)	3.65 (BF)	8.78 (BF)	11.51 (BF)	16.32 (BF)	18.61 (BF)

TABLE VII
LINK-LEVEL LOOKUP TABLE FOR THE UL DIVERSITY: SINR (IN DECIBELS; TRANSMISSION MODE)

bits/subcarrier	1 Km/h	60 Km/h	120 Km/h
1/6	-5.45 (BF)	-6.31 (BF)	-6.18 (BF)
1/4	-3.71 (BF)	-4.81 (BF)	-4.95 (BF)
1/3	-1.51 (SM)	-1.7 (SM)	-1.89 (SM)
1/2	-0.91 (BF)	-1.92 (BF)	-1.9 (BF)
1	1.31 (SM)	0.68 (SM)	1 (SM)
2	6.47 (SM)	5.81 (SM)	5.69 (SM)
3	11.5 (BF)	10.76 (BF)	10.92 (BF)
4	13.54 (SM)	12.87 (SM)	12.81 (SM)
5	18.4 (BF)	17.7 (BF)	18.5 (BF)
6	18.41 (SM)	18.03 (SM)	17.83 (SM)
8	21.52 (SM)	21.22 (SM)	21.59 (SM)
10	25.82 (SM)	25.57 (SM)	26.71 (SM)

TABLE VIII
LINK-LEVEL LOOKUP TABLE FOR THE DL DIVERSITY: SINR (IN DECIBELS; TRANSMISSION MODE)

bits/subcarrier	1 km/h	60 km/h	120 km/h
1/6	-5.65 (BF)	-8.31 (BF)	-8.90 (BF)
1/4	-4.15 (BF)	-6.69 (BF)	-7.24 (BF)
1/3	-0.75 (BFSM)	-1.87 (BFSM)	-1.64 (BFSM)
1/2	-1.45 (BF)	-3.59 (BF)	-4.43 (BF)
1	2.52 (BF)	0.26 (BF)	-0.28 (BF)
2	8.07 (BF)	6.21 (BF)	5.45 (BF)
3	12.63 (BF)	10.56 (BF)	9.83 (BF)
4	16.62 (BF)	13.79 (BF)	13.77 (BF)
5	19.77 (BF)	18.1 (BF)	17.54 (BF)
6	24.69 (DSTTD)	23.66 (BFSM)	N/A
8	27.77 (DSTTD)	27.64 (BFSM)	N/A
10	32.77 (DSTTD)	N/A	N/A

diversity gain also increases, whereas the UL CSI estimation performance in the UL sounding band is degraded. Therefore, the optimal T maximizes the sum achievable rates according to the UL SINR. Our simulation results show that, when the UL SINR in the UL sounding band is 10 and 15 dB, the optimal T is given by 6 and 9, respectively. It is also observed that the designed MU-MIMO OFDMA system has higher sum achievable rates than the MIMO OFDMA systems and the gain ranges from 11% to 86% in the DL AMC bands when T varies from 2 to 18.

C. Overall Average Cell Throughput

In this section, the system-level cell throughput is shown by performing both link-level and multicell simulations in the other bands (except for the DL AMC band). The link-level lookup tables that satisfy the FER 10^{-2} for each MIMO scheme are generated and summarized in Tables VI–VIII for the UL AMC, UL diversity, and DL diversity bands, respectively, after running the link-level simulation.[18] The considered MIMO schemes are summarized in Table IX. In the multicell simulation, it is assumed that the total number of users given by 15, nine, four, and two users move at a velocity of 1, 60, and 120 km/h, respectively. The number of the DL AMC users is given by six out of nine users who move at a velocity of 1 km/h. We focus on the physical (PHY)-layer throughput, which is the UL/DL data throughput that includes overheads, e.g., the TTG, UL control, RTG, preamble, DL-MAP, and pilots shown in Fig. 2. When the ratio of the UL/DL frame length and the AMC/diversity band are 19/20 and 1/3, respectively, and the received SINR of the UL sounding band at the BS is fixed as 15 dB according to the power control by UEs, the average cell throughput is then shown in Table X. Based on this result, we may conclude that the proposed MU-MIMO OFDMA system yields a cell throughput improvement of 22.5% compared with the conventional MIMO OFDMA system.

TABLE IX
MIMO SCHEMES FOR THE LINK-LEVEL SIMULATIONS

	Uplink	Downlink
Diversity	OL-BF, SM	OL-BF, DSTTD, OL-BFSM
AMC	OL-BF	MU-MIMO, BFSM

VI. CONCLUSION

In this paper, we have described the TDD frame and the pilots that enabled us to estimate CSI for MU-MIMO OFDMA systems where the BS and UEs are equipped with four transmitting and two receiving antennas, respectively. The UL pilots, UL sounding, DL pilots, and midamble were constructed for the estimation of UL CSI, UL CSI of sounding bands, DL CSI, and effective DL CSI, respectively. To reduce the computational complexity of MU scheduling, the simplified algorithm, which can select users and spatial modes, was also proposed. It was shown that, with a great computational complexity reduction, the performance of the proposed suboptimal TR search is almost identical to the optimal EX search. It was found that

[18]For the DL AMC band, the system-level simulation is based on the link-level lookup table generated not from each MIMO scheme but from each spatial stream, i.e., single-antenna channel. This is because both MIMO techniques, i.e., our MU-MIMO and CL-BFSM, in DL AMC bands can support multiple spatial streams, and thus, different MCS levels can be applied to each stream.

TABLE X
AVERAGE CELL THROUGHPUT WHEN THE TOTAL NUMBER OF USERS IS 15 IN UL/DL SUBFRAMES AND THE RECEIVED SINR OF THE UL SOUNDING BAND AT THE BS IS FIXED AS 15 dB BY THE UL POWER CONTROL

DL:UL	AMC:Diversity	Link	Diversity (Kbps)	AMC (Kbps)		Total throughput (Kbps)	
				MIMO	MU-MIMO	MIMO	MU-MIMO
20:19	1:3	Downlink	1802.3	5089.9	7632.9	6892.2	9435.2
		Uplink	1451.4	2957.1		4408.5	

the sum achievable rates of the proposed MU-MIMO OFDMA system increased up to 86% (at least 11%) compared with the conventional MIMO OFDMA system in the DL AMC bands. We also evaluated the overall average cell throughput, including both UL and DL subframes, and verified that the cell throughput of the proposed MU-MIMO OFDMA system increased by 22.5% compared with the conventional MIMO OFDMA system. Further investigation of the performance gain for the MU-MIMO OFDMA systems under various antenna configurations remains for future work. Suggestions for further research in this area also include designing a robust MU-MIMO OFDMA technique based on the channel estimation error.

REFERENCES

[1] I. E. Telatar, "Capacity of multiantenna Gaussian channels," *Eur. Trans. Telecommun.*, vol. 10, no. 6, pp. 585–595, Nov./Dec. 1999.

[2] G. J. Foschini, "Layered space–time architecture for wireless communication in a fading environment when using multielement antennas," *Bell Labs Tech. J.*, vol. 1, pp. 41–59, Autumn 1996.

[3] H. Weingarten, Y. Steinberg, and S. Shamai, "The capacity region of the Gaussian multiple-input–multiple-output broadcast channel," *IEEE Trans. Inf. Theory*, vol. 52, no. 9, pp. 3936–3964, Sep. 2006.

[4] Y. Sun, Y. Yang, A. D. Liveris, V. Stankovi, and Z. Xiong, "Near-capacity dirty-paper code design: A source–channel coding approach," *IEEE Trans. Inf. Theory*, vol. 55, no. 7, pp. 3013–3031, Jul. 2009.

[5] M. Stojnic, H. Vikalo, and B. Hassibi, "Rate maximization in multiantenna broadcast channels with linear preprocessing," *IEEE Trans. Wireless Commun.*, vol. 5, no. 9, pp. 2338–2342, Sep. 2006.

[6] C. B. Peel, B. M. Hochwald, and A. L. Windlehurst, "A vector-perturbation technique for near-capacity multiantenna multiuser communication—Part I: Channel inversion and regularization," *IEEE Trans. Commun.*, vol. 53, no. 1, pp. 195–202, Jan. 2005.

[7] R. L.-U. Choi, M. T. Ivrlac, R. D. Murch, and J. A. Nossek, "Joint transmit and receive multiuser MIMO decomposition approach for the downlink of multiuser MIMO systems," in *Proc. IEEE VTC*, Orlando, FL, Oct. 2003, pp. 409–413.

[8] L.-U. Choi and R. D. Murch, "A transmit preprocessing technique for multiuser MIMO systems using a decomposition approach," *IEEE Trans. Wireless Commun.*, vol. 3, no. 1, pp. 20–24, Jan. 2004.

[9] Q. H. Spencer, A. L. Swindlehurst, and M. Haardt, "Zero-forcing methods for downlink spatial multiplexing in multiuser MIMO channels," *IEEE Trans. Signal Process.*, vol. 52, no. 2, pp. 461–471, Feb. 2004.

[10] Z. Pan, K.-K. Wong, and T.-S. Ng, "Generalized multiuser orthogonal space-division multiplexing," *IEEE Trans. Wireless Commun.*, vol. 3, no. 6, pp. 1969–1973, Nov. 2004.

[11] J. Joung and Y. H. Lee, "Regularized channel diagonalization for multiuser MIMO downlink using a modified MMSE criterion," *IEEE Trans. Signal Process.*, vol. 55, no. 4, pp. 1573–1579, Apr. 2007.

[12] M. Jiang and L. Hanzo, "Multiuser MIMO-OFDM for next-generation wireless systems," *Proc. IEEE*, vol. 95, no. 7, pp. 1430–1469, Jul. 2007.

[13] N. Jindal, "MIMO broadcast channels with finite-rate feedback," *IEEE Trans. Inf. Theory*, vol. 52, no. 11, pp. 5045–5060, Nov. 2006.

[14] T. Yoo, N. Jindal, and A. Goldsmith, "Multiantenna broadcast channels with limited feedback and user selection," *IEEE J. Sel. Areas Commun.*, vol. 25, no. 7, pp. 1478–1491, Sep. 2007.

[15] P. Viswanath, D. N. C. Tse, and R. Laroia, "Opportunistic beamforming using dumb antennas," *IEEE Trans. Inf. Theory*, vol. 48, no. 6, pp. 1277–1294, Jun. 2002.

[16] M. Sharif and B. Hassibi, "On the capacity of MIMO broadcast channels with partial-side information," *IEEE Trans. Inf. Theory*, vol. 51, no. 2, pp. 506–522, Feb. 2005.

[17] G. Caire, N. Jindal, M. Kobayashi, and N. Ravindran, "Multiuser MIMO achievable rates with downlink training and channel state feedback," *IEEE Trans. Inf. Theory*, vol. 56, no. 6, pp. 2845–2866, Jun. 2010.

[18] H. Viswanathan, S. Venkatesan, and H. Huang, "Downlink capacity evaluation of cellular networks with known-interference cancellation," *IEEE J. Sel. Areas Commun.*, vol. 21, no. 5, pp. 802–811, Jun. 2003.

[19] J. Joung, E. Y. Kim, S. H. Lim, Y.-U. Jang, W.-Y. Shin, S.-Y. Chung, J. Chun, and Y. H. Lee, "Capacity evaluation of various multiuser MIMO schemes in downlink cellular environments," in *Proc. IEEE PIMRC Symp.*, Helsinki, Finland, Sep. 2006, pp. 1–5.

[20] G. Dimi and N. D. Sidiropoulos, "On downlink beamforming with greedy user selection: Performance analysis and a simple new algorithm," *IEEE Trans. Signal Process.*, vol. 53, no. 10, pp. 3857–3868, Oct. 2005.

[21] T. Yoo and A. Goldsmith, "On the optimality of multiantenna broadcast scheduling using zero-forcing beamforming," *IEEE J. Sel. Areas Commun.*, vol. 24, no. 3, pp. 528–541, Mar. 2006.

[22] Z. Shen, R. Chen, J. G. Andrews, R. W. Heath, Jr., and B. L. Evans, "Low-complexity user selection algorithms for multiuser MIMO systems with block diagonalization," *IEEE Trans. Signal Process.*, vol. 54, no. 9, pp. 3658–3663, Sep. 2006.

[23] *Worldwide Interoperability for Microwave Access (WiMAX)*, 2006. [Online]. Available: http://www.wimaxforum.org

[24] *IEEE 802.16m System Requirements, IEEE 802.16m-07/002r8*, Jan. 2009. [Online]. Available: http://wirelessman.org/tgm/

[25] S. Ahmadi, "An overview of next-generation mobile WiMAX technology," *IEEE Commun. Mag.*, vol. 47, no. 6, pp. 84–98, Jun. 2009.

[26] J. Lee, J.-K. Han, and J. Zhang, "MIMO technologies in 3GPP LTE and LTE-Advanced," *EURASIP J. Wireless Commun. Netw.*, 2009, Article ID 302092, DOI:10.1155/2009/302092.

[27] Y.-H. Jung, J.-H. Chung, C.-S. Hwang, S.-H. Nam, Y.-H. Lee, and H.-S. Park, "Pilot designing method in an uplink OFDMA system," U.S. Patent 7 710 918, May 4, 2010.

[28] F. W. Vook, Z. Zhuang, K. L. Baum, and T. A. Thomas, "Signaling methodologies to support closed-loop transmit processing in TDD-OFDMA," IEEE Std. C802.16e-04/103, May 2004.

[29] F. W. Vook, Z. Zhuang, K. L. Baum, T. A. Thomas, M. Cudak, I. Sutskover, D. Ben-Eli, U. Perlmutter, Y. Leiba, Y. Segal, Z. Hadad, I. Kitroser, E. Shasha, A. Kerr, J. Jang, and W. Roh, "Uplink channel sounding for TDD OFDMA," IEEE Std. C802.16e-04/263r3, Aug. 2004.

[30] F. W. Vook, X. Zhuang, K. L. Baum, T. A. Thomas, P. Sartori, Z. Hadad, and W. Tong, "Improvements to the uplink channel sounding signaling for OFDMA," IEEE Std. C802.16e-04/422r4, Jan. 2005.

[31] IEEE Air Interface for Fixed and Mobile Broadband Wireless Access Systems, IEEE Std. P802.16e/D12, 2005.

[32] F. Jelinek, "Fast sequential decoding algorithm using a stack," *IBM J. Res. Develop.*, vol. 13, no. 6, pp. 675–685, Nov. 1969.

[33] Y.-U. Jang, H. M. Kwon, and Y. H. Lee, "Adaptive mode selection for multiuser MIMO downlink systems," in *Proc. IEEE VTC*, Melbourne, Australia, May 2006, pp. 2003–2007.

[34] B. Hassibi and B. M. Hochwald, "How much training is needed in multiple-antenna wireless links," *IEEE Trans. Inf. Theory*, vol. 49, no. 4, pp. 951–963, Apr. 2003.

[35] S. H. Simon and A. L. Moustakas, "Optimizing MIMO antenna systems with channel covariance feedback," *IEEE J. Sel. Areas Commun.*, vol. 21, no. 3, pp. 406–417, Apr. 2003.

[36] J. Joung, E.-R. Jeong, and Y. H. Lee, "A computationally efficient criterion for antenna shuffling in DSTTD systems," *IEEE Commun. Lett.*, vol. 11, no. 9, pp. 732–734, Sep. 2007.

[37] I. H. Kim, K. Lee, and J. Chun, "A MIMO antenna structure that combines transmit beamforming and spatial multiplexing," *IEEE Trans. Wireless Commun.*, vol. 6, no. 3, pp. 775–779, Mar. 2007.

[38] T. Kwon, S. Cho, H. Lee, S. Choi, J. Kim, S. Yun, W.-H. Park, D.-H. Cho, and K. Kim, "Design and implementation of a simulator based on a cross-layer protocol between MAC and PHY layers in a WiBro compatible IEEE 802.16e OFDMA systems," *IEEE Commun. Mag.*, vol. 43, no. 12, pp. 136–146, Dec. 2005.
[39] M. Morelli and U. Mengali, "A comparison of pilot-aided channel estimation methods for OFDM systems," *IEEE Trans. Signal Process.*, vol. 49, no. 12, pp. 3065–3073, Dec. 2001.
[40] M. Guillaud, D. T. M. Slock, and R. Knopp, "A practical method for wireless channel reciprocity exploitation through relative calibration," in *Proc. ISSPA*, Sydney, Australia, Aug. 2005, pp. 403–406.
[41] R. Negi and J. Cioffi, "Pilot tone selection for channel estimation in a mobile OFDM system," *IEEE Trans. Consum. Electron.*, vol. 44, no. 3, pp. 1122–1128, Aug. 1998.
[42] G. H. Golub and C. F. V. Loan, *Matrix Computations*, 3rd ed. Baltimore, MD: Johns Hopkins Univ. Press, 1996..
[43] 3GPP2/TSG-c.R1002 Third-Generation Partnership Project 2, 2003. [Online]. Available: http://www.3gpp2.org/.
[44] T. S. Rappaport, *Wireless Communications—Principles and Practice*. Upper Saddle River, NJ: Prentice-Hall, 1996.

Yong-Up Jang (S'03–M'10) received the B.S. degree in electrical and computer engineering from Hanyang University, Seoul, Korea, in 2003 and the Ph.D. degree in electrical engineering from the Korea Advanced Institute of Science and Technology (KAIST), Daejeon, Korea, in 2010.

From March 2010 to August 2010, he was a Postdoctoral Researcher with the KAIST Institute for Information Technology Convergence, where he has been a Senior Researcher since September 2010. His research interests include cooperative relay networks, multiuser scheduling, multiuser multiple-input multiple-output, and cognitive radio networks.

Jingon Joung (S'04–M'07) received the B.S. degree in electrical engineering from Yonsei University, Seoul, Korea, in 2001 and the M.S. degree in electrical engineering and the Ph.D. degree in computer science from the Korea Advanced Institute of Science and Technology (KAIST), Daejeon, Korea, in 2003 and 2007, respectively.

From March 2007 to August 2008, he was a Postdoctoral Research Scientist with the Department of Electrical Engineering, KAIST. From April 2007 to August 2008, he was a Commissioned Researcher with Lumicomm Inc., Daejeon. From October 2008 to September 2009, he was a Postdoctoral Fellow with the Department of Electrical Engineering, University of California, Los Angeles. Since October 2009, he has been a Researcher with the Institute for Infocomm Research, Agency for Science, Technology and Research, Singapore. His research activities include multiuser systems, multiple-input–multiple-output communications, and cooperative systems.

Dr. Joung is the recipient of the Gold Prize at the Intel–Information Technology Research Center Student Paper Contest in 2006.

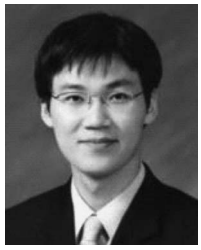

Won-Yong Shin (S'02–M'08) received the B.S. degree in electrical engineering from Yonsei University, Seoul, Korea in 2002 and the M.S. degree in electrical engineering and the Ph.D. degree in computer science from the Korea Advanced Institute of Science and Technology (KAIST), Daejeon, Korea, in 2004 and 2008, respectively.

From September 2008 to April 2009, he was with the Brain Korea Institute and CHiPS, KAIST, as a Postdoctoral Fellow. From August 2008 to April 2009, he was with Lumicomm Inc., Daejeon, as a Visiting Researcher. From February to April 2008, he was a Visiting Scholar with Harvard University, Cambridge, MA. Since May 2009, he has been with the School of Engineering and Applied Sciences, Harvard University, where he is currently a Postdoctoral Fellow. His research interests include information theory, communications, and signal processing and their applications to ocean information technology.

Eui-Rim Jeong (M'04) received the B.S., M.S., and Ph.D. degrees in electrical engineering from the Korea Advanced Institute of Science and Technology, Daejeon, Korea, in 1995, 1997, and 2001, respectively.

He is currently an Assistant Professor with the Division of Information Communication and Computer Engineering, Hanbat National University, Daejeon. His research interests include relay networks, communication signal processing, and digital predistortion.